Dihedral 'Star' Tensegrity Structures

J.Y. Zhang [a,*] S.D. Guest [b] R. Connelly [c] M. Ohsaki [a]

[a] *Dept. of Architecture and Architectural Engineering, Kyoto University, Japan*

[b] *Dept. of Engineering, University of Cambridge, United Kingdom*

[c] *Dept. of Mathematics, Cornell University, USA*

Abstract

This paper presents conditions for self-equilibrium and super stability of dihedral 'star' tensegrity structures, based on their dihedral symmetry. It is demonstrated that the structures are super stable if and only if they have an odd number of struts, and the struts are as close as possible to each other. Numerical investigations show that their prestress stability is sensitive to the geometry realisation.

Key words: Tensegrity structure; Dihedral symmetry; Block-diagonalisation; Self-equilibrium; Stability.

1. Introduction

In this paper, we describe dihedral 'star' tensegrity structures which we derive from the classic dihedral prismatic tensegrity structures. The horizontal cables in each of the two parallel circles containing the nodes in a prismatic structure are replaced by a star of cables in a 'star' structure, with a new centre node. An example 'star' structure is shown in Fig. 1(b), along with the parent prismatic structure in Fig. 1(a). Also shown in Fig. 1(c) is an embellishment of the structure, where there exists a centre member connected to the two centre nodes.

There is a clear link between the star structures, and the parent prismatic structures that were studied by Connelly and Terrell (1995); Zhang *et al.* (2008a). Indeed, we shall see that the equilibrium positions of the nodes, and self-stress forces in the vertical cables and the struts, are identical in the star and prismatic structures, as long as there is no centre member. However, the star structure has many more infinitesimal mechanisms than its parent prismatic structure: at each of the boundary nodes, a strut is in equilibrium with two cables, all of which must therefore lie in a plane; thus, out-of-plane movement of the node must be an infinitesimal mechanism, and there are at least six infinitesimal

* Dept. of Architecture and Architectural Engineering, Kyoto University, Kyoto-daigaku Katsura, Nishikyo, Kyoto 615-8540, Japan.
Email: is.zhang@archi.kyoto-u.ac.jp

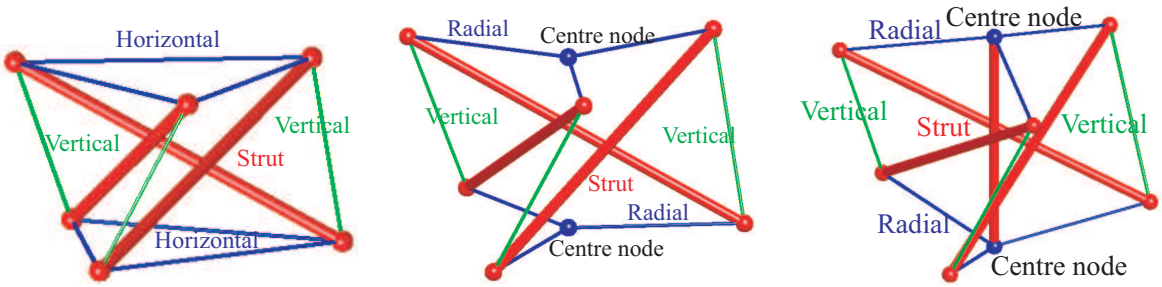

(a) prismatic (b) star (c) star with centre member

Fig. 1. Tensegrity structures that are of the same dihedral symmetry $\mathbf{D}_3$. The thick lines represent struts, and the thin lines represent cables.

mechanisms—in fact there is another infinitesimal mechanism corresponding to the existence of one self-stress mode of the structure By contrast, there is only one non-rigid-body infinitesimal mechanism in the prismatic tensegrity structure. Despite this, we will show that many dihedral star tensegrity structures can be stable, and further, that in some cases they are *super* stable, which implies that they are stable for any level of self-stress, independent of the stiffness of the members.

Following this introduction, the paper is organized as follows: Section 2 uses the symmetry of a star structure to find its configuration and self-stress forces in the state of self-equilibrium. Section 3 presents the necessary and sufficient condition for an 'indivisible' structure. Section 4 block-diagonalises the force density matrix and finds the condition, in terms of connectivity of vertical cables, for super stability of the star structures; prestress stability of the structures that are not super stable is numerically investigated. Section 5 briefly concludes the study on the star structures, and discusses the stability properties of those with centre members.

2. Configuration

In this section, we introduce the connectivity and geometry of a general star structure, and find the internal forces that equilibrate every node. The structure has dihedral symmetry, and this symmetry allows us to calculate symmetric state of self-stress by considering the equilibrium equations of only representative nodes.

2.1 Symmetry and connectivity

We are considering star tensegrity structures that have dihedral symmetry, denoted $\mathbf{D}_n$ (in the Schoenflies notation): there is a single major n-fold rotation (C_n^i) axis, which we assume is the vertical, z-axis, and n 2-fold rotation ($C_{2,j}$) axes perpendicular to this major axis. In total there are $2n$ symmetry operations. A star structure has the same apperance before and after the transformation by applying any of these symmetry operations.

Consider a specific set of elements (nodes or members) of a structure with symmetry G. If one element in a set can be transformed to all of the other elements of that set by the symmetry operations in G, then this set of elements are said to belong to the same *orbit*. A structure can have several different orbits of elements.

In contrast to prismatic structures, which have only one orbit of nodes, there are two orbits of nodes in star structures—boundary nodes and centre nodes, as shown in Fig. 2:

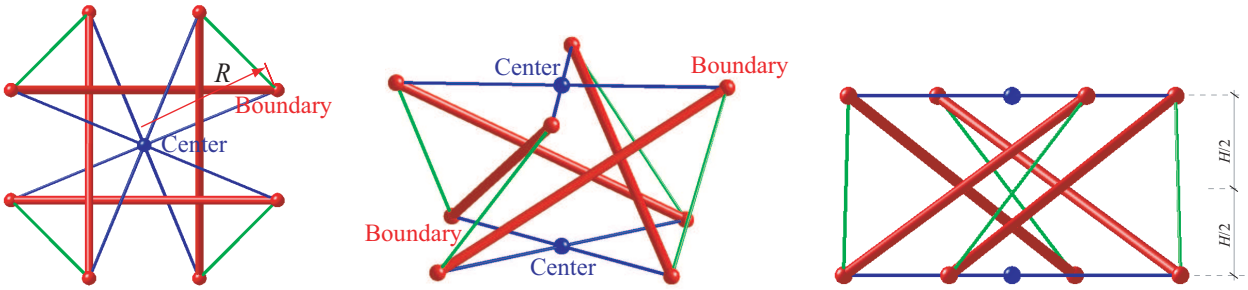

(a) top (b) perspective (c) side

Fig. 2. The dihedral star tensegrity structure $\mathbf{D}_4^1$. R and H are the radius of the circle of boundary nodes and height of the structure, respectively.

- There are $2n$ 'boundary' nodes arranged in two horizontal circles of radius R around the vertical z-axis; there is a one-to-one correspondence between the boundary nodes and the symmetry operations. (When there is a one-to-one correspondence between elements and symmetry operations, the orbit is called a *regular orbit*).
- There are two 'centre' nodes that lie on the centres of the two horizontal circles; the cyclic (n-fold) rotation operations do not change the locations of these nodes, while the 2-fold rotation operations swap their positions.

Thus, there are in total $2n+2$ nodes. The two horizontal circles containing the boundary nodes are at $z = \pm H/2$, and the centre nodes are also at $z = \pm H/2$, as shown in Fig. 2(c).

There are three orbits of members: radial cables, vertical cables and struts. The members in each orbit have the same length and internal force, and therefore, the same force density (ratio of internal force to length). Each of the boundary nodes in a circle is connected by a 'radial' cable to a centre node. Hence, there are $2n$ radial cables, and each symmetry operation transforms a radial cable into one of the other radial cables; i.e., there is a one-to-one correspondence between the radial cables and the symmetry operations (the radial cables form a regular orbit). Each boundary node is connected by a strut and a 'vertical' cable to boundary nodes in the other circle. Thus, there are only n vertical cables, and n struts: there is a one-to-two correspondence between the vertical cables (or struts) and the symmetry operations. Each vertical cable and strut intersects one of the 2-fold horizontal rotation axes, and this 2-fold operation transforms this vertical cable (or strut) into itself.

It is possible to have different connectivities of the vertical cables and struts for any $n > 3$. We use the notation $\mathbf{D}_n^v$ to describe the connectivity of a star tensegrity with $\mathbf{D}_n$ symmetry, where v describes the connectivity of the vertical cables, assuming that connectivity of struts is fixed. The boundary nodes in the upper and lower circles are respectively numbered as $N_0, N_1 \ldots, N_{n-1}$ and $N_n, N_{n+1} \ldots, N_{2n-1}$, and the upper and lower centre nodes are numbered as N_{2n} and N_{2n+1}, respectively. We describe the connectivity of a reference node N_0 as follows—all other connections are then defined by the symmetry.

(1) Without loss of generality, we assume that a strut connects node N_0 in the upper circle to node N_n in the lower circle.
(2) A radial cable in the upper circle connects node N_0 to the centre node N_{2n}, and a radial cable in the lower circle connects node N_n to the centre node N_{2n+1}.

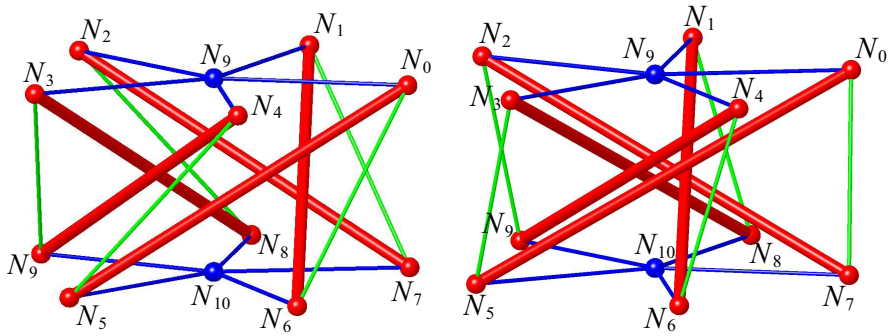

(a) $\mathbf{D}_5^1$ $\mathbf{D}_5^2$

Fig. 3. The nodal numbering of two example structures with $\mathbf{D}_5$ symmetry.

(3) A vertical cable connects node N_0 in the upper circle to node N_{n+v} in the lower circle. We restrict $1 \leq v \leq n/2$ (choosing $n/2 \leq v \leq n$ would give essentially the same set of structures, but in left-handed versions).

The numbering of nodes of two example structures with $\mathbf{D}_5$ symmetry, $\mathbf{D}_5^1$ and $\mathbf{D}_5^2$, is shown in Fig. 3. Node N_0 is connected by a strut to node N_5, and by a cable to node N_6 for $\mathbf{D}_5^1$, and to node N_7 for $\mathbf{D}_5^2$.

2.2 Symmetric state of self-stress

Because of the high symmetry of the star structures, we only need to consider the equilibrium of one reference node from each orbit, to find the symmetric state of self-stress. Thus we consider the equilibrium of one boundary node, and one center node, in the absence of external forces.

Consider the boundary nodes first. Take one of them, for example node N_0 in the upper circle, as the *reference node* and let $\mathbf{x}_0 \in \Re^3$ denote its coordinates in three-dimensional space. The coordinates of the other two boundary nodes in the lower circle, connected to the reference node by the strut and vertical cable, respectively, are denoted by $\mathbf{x}_s$ and $\mathbf{x}_v$; the coordinates of the centre node in the upper circle is denoted by $\mathbf{x}_c$.

Since the boundary nodes are in the same orbit, the reference node $\mathbf{x}_0$ can be transformed to the boundary nodes $\mathbf{x}_s$ and $\mathbf{x}_v$ by the proper 2-fold rotations written in the form of transformation matrices $\mathbf{R}_s$ and $\mathbf{R}_v$:

$$\begin{aligned} \mathbf{x}_s &= \mathbf{R}_s \mathbf{x}_0, \\ \mathbf{x}_v &= \mathbf{R}_v \mathbf{x}_0. \end{aligned} \tag{1}$$

where $\mathbf{R}_s$ and $\mathbf{R}_v$ are defined as

$$\mathbf{R}_s = \begin{bmatrix} 1 & 0 & 0 \\ 0 & -1 & 0 \\ 0 & 0 & -1 \end{bmatrix}, \quad \mathbf{R}_v = \begin{bmatrix} C_v & S_v & 0 \\ S_v & -C_v & 0 \\ 0 & 0 & -1 \end{bmatrix}, \tag{2}$$

using the notation $C_v = \cos(2v\pi/n)$ and $S_v = \sin(2v\pi/n)$. (Note that here we have effectively chosen a particular handedness for the structure with our choice of a positive direction for rotation in $\mathbf{R}_v$, and we have chosen that the reference node must be connected to a strut that intersects the x-axis by our choice of $\mathbf{R}_s$.)

The coordinates $\mathbf{x}_c$ of the center node in the upper circle is already known, if the height H of the structure is given:

$$\mathbf{x}_c = \begin{bmatrix} 0 \\ 0 \\ H/2 \end{bmatrix}. \tag{3}$$

Denote the force densities (internal force to length ratios) of the strut, vertical and radial cables as q_s, q_v and q_r, respectively. The equilibrium of the reference node, in the absence of external force, is

$$q_s(\mathbf{x}_s - \mathbf{x}_0) + q_v(\mathbf{x}_v - \mathbf{x}_0) + q_r(\mathbf{x}_c - \mathbf{x}_0) = \mathbf{0}. \tag{4}$$

From Eq. (2), Eq. (4) can be rewritten as

$$\bar{\mathbf{E}}\mathbf{x}_0 + q_r\mathbf{x}_c = \mathbf{0}, \tag{5}$$

where

$$\bar{\mathbf{E}} = \begin{bmatrix} \bar{\mathbf{E}}_1 & \mathbf{O} \\ \mathbf{O} & \bar{\mathbf{E}}_2 \end{bmatrix} = -\begin{bmatrix} q_v(1-C_v)+q_r & -q_vS_v & 0 \\ -q_vS_v & 2q_s+q_v(C_v+1)+q_r & 0 \\ 0 & 0 & 2q_s+2q_v+q_r \end{bmatrix}, \tag{6}$$

where $\bar{\mathbf{E}}_1 \in \Re^{2\times 2}$ and $\bar{\mathbf{E}}_2 \in \Re^{1\times 1}$. Note that $\bar{\mathbf{E}}$ is in fact part of the symmetry-adapted force density matrix presented later in the paper.

Using Eq. (3), Eq. (4) can be separated into the following two independent equations

$$\bar{\mathbf{E}}_1\bar{\mathbf{x}}_0 = \mathbf{0} \tag{7}$$

and

$$\bar{\mathbf{E}}_2 H/2 + q_r H/2 = (-2q_s - 2q_v - q_r)H/2 + q_r H/2 = 0, \tag{8}$$

where the vector $\bar{\mathbf{x}}_0 \in \Re^2$ denotes the coordinates of the reference node in xy-plane. Because $H \neq 0$, Eq. (8) gives

$$q_v = -q_s. \tag{9}$$

In order to have non-trivial coordinates ($\bar{\mathbf{x}}_0 \neq \mathbf{0}$) in xy-plane, $\bar{\mathbf{E}}_1$ should be singular; i.e., its determinant should be zero. Hence, we have

$$q_r^2 + q_v^2(C_v - 1) = 0, \tag{10}$$

where Eq. (9) has been applied. The force density q_r of the radial cable should be positive that can be solved as

$$q_r = +q_v\sqrt{2(1-C_v)}. \tag{11}$$

Thus we have found force densities in the members that allow the structure to be in self-equilibrium — equilibrium of the centre nodes is automatically satisfied. For the reference node, the coordinate $\bar{\mathbf{x}}_0$ in the xy-plane lies in the null-space of $\bar{\mathbf{E}}_1$ and the coordinate in z-direction is $H/2$, giving

$$\mathbf{x}_0 = \frac{R}{R_0}\mathbf{r} + \frac{H}{2}\mathbf{h} = \frac{R}{R_0}\begin{bmatrix} C_v - 1 + \sqrt{2-2C_v} \\ S_v \\ 0 \end{bmatrix} + \frac{H}{2}\begin{bmatrix} 0 \\ 0 \\ 1 \end{bmatrix}, \tag{12}$$

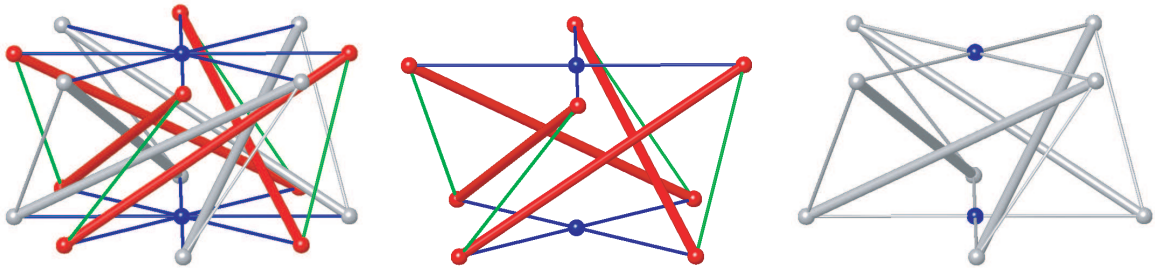

(a) original structure (b) substructure $\mathbf{D}_4^1$ (c) substructure $\mathbf{D}_4^1$

Fig. 4. Divisible dihedral star tensegrity structure $\mathbf{D}_8^2$. Any of the two substructures $\mathbf{D}_4^1$ can rotate about the z-axis without mechanical influence on the other.

where $R_0(= 2\sqrt{(1-C_v)(1-S_{v/2})})$ is the norm of $\mathbf{r}$. Thus, R is the arbitrary radius of the circles containing the boundary nodes, and the complexity of Eq. (12) arises from our choice that the strut connected to the reference node should intersect the x-axis.

3. Divisibility

The previous section has found equilibrium configurations for dihedral star tensegrity structures, but these structures may be stable or unstable. Before stability investigation in the next section, we present the condition for indivisible structures, since the divisible structures should have been considered in the simpler substructures with less nodes and members.

Note that, unlike prismatic tensegrity structures catalogued by Zhang *et al.* (2008a), the 'star' tensegrity structures are never strictly divisible — all elements of the structure are connected. Despite this, it is possible for parts of the structure to act independently of one another of one particular set of relative motions — rotations around the z-axis. Thus we define a dihedral star tensegrity to be *divisible* if the members and nodes can be separated into two or more identical substructures that are only interconnected by being pinned together at the common centre nodes. Rotation of one substructure about z-axis has no mechanical influence on other substructures. Hence, the divisible structure has a finite mechanism, and therefore cannot be stable. As an example, the structure $\mathbf{D}_8^2$ shown in Fig. 4(a) is divisible — it can be separated into two identical structures $\mathbf{D}_4^1$ as shown in Figs. 4(b) and (c). The struts and vertical cables in each substructure connect one to another to form a closed circuit, so that the substructures are indivisible.

From the labels of nodes and definition of connectivities of struts and vertical cables, node N_i in the upper circle is connected to node N_{n+i+v} by a vertical cable; node N_{n+i+v} is connected to node N_{i+v} by a strut; node N_{i+v} is connected to N_{n+i+2v} by a vertical cable, and so on. Eventually, we must return back to the starting node N_i. If we stop when the linkage returns back to the starting node N_i for the first time, the boundary nodes in the upper circle in the linkage can be listed as follows

$$N_i \to N_{i+v} \to N_{i+2v} \to \cdots \to N_{i+jv-mn} (\equiv N_i). \tag{13}$$

The numbers j and m indicate the number of boundary nodes in the upper circle that have been visited, and the number of circuits around the z-axis, respectively.

To return to the starting node N_i, we have $i + jv - mn = i$, and hence

$$jv = mn. \tag{14}$$

We must have integer solution for j and m, which we can write as $j = n/D$, $m = v/D$, where D is any common divisor of n and v. If the structure is indivisible, we should have visited all n boundary nodes in the upper circle. Thus, the minimum solution for j for an indivisible structure is $j = n$, from which we must have that D can only be 1. In summary, the necessary and sufficient indivisibility condition for a star structure is that v and n have no common divisor except 1.

4. Stability

This section will investigate the stability of the star tensegrity structures. We will introduce the ideas of super stability and prestress stability, and show which structures are super stable, and which are prestress stable for varying ratios of R/H.

4.1 Symmetry-adapted force density matrix

A super stable star tensegrity structure is guaranteed to be stable for any arbitrary R and H, and any level of prestress. The force density matrix (sometimes called the 'small' stress matrix, for example in Guest (2006)) is critical to super stability of a tensegrity structure.

The force density matrix $\mathbf{E} \in \Re^{(2n+2)\times(2n+2)}$ is a symmetric matrix, defined using the force densities: Let $\mathcal{I}$ denote the set of members connected to free node i, the (i, j)-component $\mathbf{E}_{(i,j)}$ of $\mathbf{E}$ is given as

$$\mathbf{E}_{(i,j)} = \begin{cases} \sum\limits_{k\in\mathcal{I}} q_k & \text{for } i = j, \\ -q_k & \text{if nodes } i \text{ and } j \text{ are connected by member } k, \\ 0 & \text{if nodes } i \text{ and } j \text{ are not connected,} \end{cases} \tag{15}$$

where q_k denotes the force density of member k.

Connelly (1982) and Zhang and Ohsaki (2006) presented the equivalent sufficient conditions for the super stability of a tensegrity structure:

(1) The force density matrix has the minimum rank deficiency of four for a three-dimensional structure;
(2) The force density matrix is positive semi-definite;
(3) The member directions do not lie on a conic at infinity (Connelly, 1982), or equivalently, the geometry matrix is full-rank (Zhang and Ohsaki, 2006).

Note that the last two are also the necessary conditions for super stable structures. Since the third condition is always satisfied for indivisible star structures, we need only to consider the first two conditions, both of which are in terms of the force density matrix.

We can simplify the calculation of the stability properties of the structure by considering the force density matrix written, using symmetry-adapted coordinates, in a way that closely mirrors the treatment in Zhang *et al.* (2008a,b). The structure of this matrix can be determined considering the permutation representation of the nodes, written in terms of irreducible representations. For a dihedral group $\mathbf{D}_n$, the irreducible representations

are denoted as A_1, A_2, B_1, B_2, E_k ($k = \{1, \ldots, p\}$), where B_1 and B_2 only exist for n even and

$$p = \begin{cases} (n-1)/2, & \text{for } n \text{ odd}, \\ (n-2)/2, & \text{for } n \text{ even}. \end{cases} \tag{16}$$

A_1, A_2, B_1, B_2 are one-dimensional and E_k are two-dimensional representations. Tables of irreducible representations will be found in Altmann and Heizig (1994), for instance.

The permutation representation of the nodes can be calculated separately for the two orbits of nodes. The boundary nodes form a regular orbit, and hence the representation is the regular representation, consisting of d copies of each d-dimensional irreducible representation:

$$\Gamma_\sigma(N^b) = A_1 + A_2 + (B_1 + B_2 +) \sum_{k=1}^{p} 2E_k. \tag{17}$$

The two centre nodes are left in places by any rotation about the z-axis, but swapped by any dihedral (2-fold) rotation, and hence the representation is

$$\Gamma_\sigma(N^c) = A_1 + A_2. \tag{18}$$

Representation of all nodes $\Gamma_\sigma(N)$ can then be summarised as

$$\Gamma_\sigma(N) = \Gamma_\sigma(N^b) + \Gamma_\sigma(N^b) = 2A_1 + 2A_2 + (B_1 + B_2) + \sum_{k=1}^{p} 2E_k, \tag{19}$$

which characterises the structure of the symmetry-adapted force density matrix $\tilde{\mathbf{E}}$. As described in Zhang *et al.* (2008b), $\tilde{\mathbf{E}}$ can be written as

$$\underset{2n\times 2n}{\tilde{\mathbf{E}}} = \begin{bmatrix} \underset{2\times 2}{\tilde{\mathbf{E}}^{A_1}} & & & & & & & & & \\ & \underset{2\times 2}{\tilde{\mathbf{E}}^{A_2}} & & & & & & & & \\ & & (\underset{1\times 1}{\tilde{\mathbf{E}}^{B_1}}) & & & & & & & \\ & & & (\underset{1\times 1}{\tilde{\mathbf{E}}^{B_2}}) & & & & & & \\ & & & & \underset{2\times 2}{\tilde{\mathbf{E}}^{E_1}} & & & & & \\ & & & & & \underset{2\times 2}{\tilde{\mathbf{E}}^{E_1}} & & & & \\ & & \mathbf{O} & & & & \ddots & & & \\ & & & & & & & \underset{2\times 2}{\tilde{\mathbf{E}}^{E_p}} & & \\ & & & & & & & & \underset{2\times 2}{\tilde{\mathbf{E}}^{E_p}} & \end{bmatrix}, \tag{20}$$

which is simply written as $\tilde{\mathbf{E}} = \tilde{\mathbf{E}}^{A_1} \oplus \tilde{\mathbf{E}}^{A_2} \oplus (\tilde{\mathbf{E}}^{B_1} \oplus \tilde{\mathbf{E}}^{B_2}) \oplus \tilde{\mathbf{E}}^{E_1} \oplus \ldots \oplus \tilde{\mathbf{E}}^{E_p}$.

All of the results can be directly found according to Zhang *et al.* (2008b), *except* the A_1 and A_2 blocks where the centre nodes contribute. Those blocks are given as

$$\tilde{\mathbf{E}}^{A_1} \oplus \tilde{\mathbf{E}}^{A_2} = \mathbf{T}\mathbf{E}\mathbf{T}^\top, \tag{21}$$

where the transformation matrix $\mathbf{T}(\in \Re^{4\times(2n+2)})$ is constructed from the characters of A_1 and A_2 representations:

$$\mathbf{T} = \begin{bmatrix} \mathbf{T}_b^{A_1}/\sqrt{2n} \\ \mathbf{T}_c^{A_1}/\sqrt{2} \\ \mathbf{T}_b^{A_2}/\sqrt{2n} \\ \mathbf{T}_c^{A_2}/\sqrt{2} \end{bmatrix}, \text{ where}$$

$$\begin{bmatrix} \mathbf{T}_b^{A_1} \\ \mathbf{T}_c^{A_1} \\ \mathbf{T}_b^{A_2} \\ \mathbf{T}_c^{A_2} \end{bmatrix} = \left[\begin{array}{cccc|cccc|cc} 1 & 1 & \dots & 1 & 1 & 1 & \dots & 1 & 0 & 0 \\ 0 & 0 & \dots & 0 & 0 & 0 & \dots & 0 & 1 & 1 \\ 1 & 1 & \dots & 1 & -1 & -1 & \dots & -1 & 0 & 0 \\ 0 & 0 & \dots & 0 & 0 & 0 & \dots & 0 & 1 & -1 \end{array}\right], \quad (22)$$

and $\mathbf{T}_b^{A_1}$, $\mathbf{T}_b^{A_2}$, $\mathbf{T}_c^{A_1}$, $\mathbf{T}_c^{A_2}$ ($\in \Re^{2n+2}$) are row vectors. The first n columns in $\mathbf{T}$ correspond to the n 'top' boundary nodes, the next n columns correspond to n 'bottom' boundary nodes, and the last two columns correspond to the two centre nodes.

The blocks of the symmetry-adapted force density matrix $\tilde{\mathbf{E}}$ are summarised as follows.

$$\tilde{\mathbf{E}}^{A_1} = \begin{bmatrix} q_r & -\sqrt{n}q_r \\ -\sqrt{n}q_r & nq_r \end{bmatrix},$$

$$\tilde{\mathbf{E}}^{A_2} = \begin{bmatrix} 2(q_v+q_s)+q_r & -\sqrt{n}q_r \\ -\sqrt{n}q_r & nq_r \end{bmatrix} = \begin{bmatrix} q_r & -\sqrt{n}q_r \\ -\sqrt{n}q_r & nq_r \end{bmatrix},$$

$$\tilde{\mathbf{E}}^{B_1} = q_r - q_s + (-1)^{v+1}q_v = q_r + q_v + (-1)^{v+1}q_v,$$

$$\tilde{\mathbf{E}}^{B_2} = q_r + q_s + (-1)^{v}q_v = q_r - q_v + (-1)^{v}q_v,$$

$$\begin{aligned} \tilde{\mathbf{E}}^{E_k} &= \begin{bmatrix} (q_r+q_v+q_s) - q_vC_{kv} - q_s & -q_vS_{kv} \\ -q_vS_{kv} & (q_r+q_v+q_s) - q_vC_{kv} + q_s \end{bmatrix} \\ &= \begin{bmatrix} q_r + q_v(1-C_{kv}) & -q_vS_{kv} \\ -q_vS_{kv} & q_r - q_v(1-C_{kv}) \end{bmatrix}, \end{aligned} \quad (23)$$

where the relation $q_v = -q_s$ from Eq. (9) has been used.

4.2 Super stability

When the conditions on equilibrium given in Section 2 are satisfied, the symmetry-adapted force density matrix will have a rank deficiency of four; each of the A_1, A_2 and (two) E_1 blocks are rank-deficient by one. To ensure a super stable structure, these blocks must be positive semi-definite and the other blocks must be positive definite. This subsection investigates when this is the case.

$\tilde{\mathbf{E}}^{A_1}$ and $\tilde{\mathbf{E}}^{A_2}$ have eigenvalues

$$\lambda_1^{A_1} = \lambda_1^{A_2} = 0 \text{ and } \lambda_2^{A_1} = \lambda_2^{A_2} = (n+1)q_r > 0, \quad (24)$$

and hence are positive semi-definite.

B_1 and B_2 exist only for n even, and v is odd for an indivisible structure. Hence, substituting Eqs. (9) and (11) to Eq. (23), we have

$$\lambda^{B_1} = \tilde{\mathbf{E}}^{B_1} = q_r - q_s + (-1)^{v+1}q_v = q_r - q_s + q_v = q_v\left(2 + \sqrt{2(1-C_v)}\right), \quad (25)$$

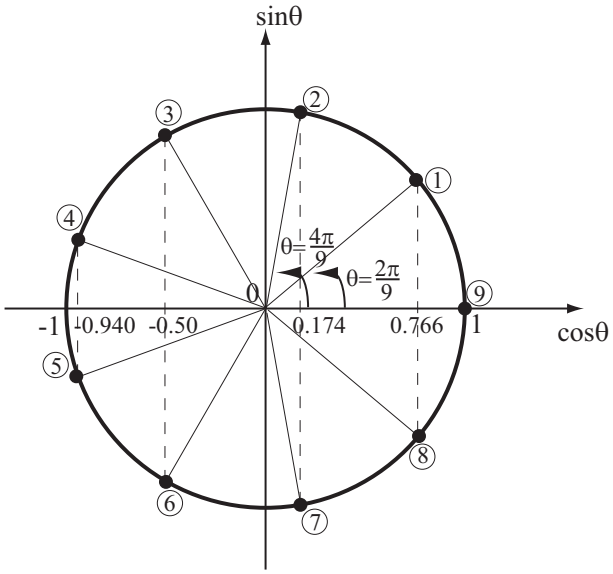

Fig. 5. Cosine corresponding to the connectivity of vertical cables v ($n = 9$).

and

$$\lambda^{B_2} = \tilde{\mathbf{E}}^{B_2} = q_r + q_s + (-1)^v q_v = q_r + q_s - q_v = q_v \left(-2 + \sqrt{2(1 - C_v)}\right). \tag{26}$$

Thus $\tilde{\mathbf{E}}^{B_1} > 0$, and is positive definite, while $\tilde{\mathbf{E}}^{B_2} \leq 0$. In fact the equality only holds if $v = n/2$, and hence for an indivisible structure ($v \neq n/2$), $\tilde{\mathbf{E}}^{B_2} < 0$, and is thus negative definite. Therefore, for n even, dihedral star tensegrity structures are never super stable.

We will now consider indivisible structures with n odd to find the super stability condition. The two eigenvalues of $\tilde{\mathbf{E}}^{E_k}$ are

$$\begin{aligned} \tfrac{1}{q_v}\lambda_1^{E_k} &= \sqrt{2(1 - C_v)} + \sqrt{2(1 - C_{kv})} > 0, \\ \tfrac{1}{q_v}\lambda_2^{E_k} &= \sqrt{2(1 - C_v)} - \sqrt{2(1 - C_{kv})}. \end{aligned} \tag{27}$$

For $k = 1$, we have $\lambda_2^{E_1} = 0$ as expected for the equilibrium condition. Thus, for $n = 3$ where $k > 1$ does not exist, the dihedral star tensegrity structure is super stable.

For $n > 4$, we must consider $\tilde{\mathbf{E}}^{E_k}$ for $k > 1$. For a super stable tensegrity, $\tilde{\mathbf{E}}^{E_k}$ for all $1 < k \leq p = (n - 1)/2$ must be positive definite; i.e., $\lambda_2^{E_k}$ must be positive; and hence, from Eq. (27) we require

$$C_{kv} > C_v, \quad \text{for all} \quad 1 < k \leq (n - 1)/2. \tag{28}$$

Each of C_{jv} ($j \in \{1, \ldots, (n - 1)/2\}$) takes one of the value in the following list with n elements

$$\left\{\cos\frac{1}{n}2\pi, \cos\frac{2}{n}2\pi, \ldots, \cos\frac{n}{n}2\pi\right\}. \tag{29}$$

The nine cosine values, four of which duplicate, for the case $n = 9$ is illustrated in Fig. 5, where the horizontal and vertical axes respectively denote cosine and sine values of a specific angle θ.

Note that $\cos\frac{i}{n}2\pi = \cos\frac{n-i}{n}2\pi$; moreover, $C_{jv} \neq \cos 2\pi$ holds, because v and n have no common divisor except 1 for an indivisible structure and $1 \leq j \leq (n - 1)/2$. Thus, the

list can be condensed as follows with $p = (n-1)/2$ elements

$$\left\{\cos\frac{1}{n}2\pi, \cos\frac{2}{n}2\pi, \ldots, \cos\frac{n-1}{2n}2\pi\right\}, \tag{30}$$

where

$$\cos\frac{1}{n}2\pi > \cos\frac{2}{n}2\pi > \ldots > \cos\frac{n-1}{2n}2\pi. \tag{31}$$

It is apparent that $v = (n-1)/2 = p$ will lead to $C_{kv} \geq C_v$ for $1 < k \leq p$. However, this is the necessary and sufficient condition only if each of C_{jv} ($j \in \{1, \ldots, (n-1)/2\}$) has one-to-one correspondence to the elements in the condensed list in Eq. (30), as proved in Lemma 1.

Lemma 1: Each of C_{jv} ($j \in \{1, \ldots, (n-1)/2\}$) has one-to-one correspondence with the elements in the condensed list in Eq. (30), for an indivisible structure with n odd.
Proof.

To prove the lemma, we need only to show that the relation $C_{k_1 v} \neq C_{k_2 v}$ holds for $k_1 \neq k_2$.

The relation $C_{k_1 v} = C_{k_2 v}$ holds only if

$$\frac{k_1 v - m_1 n}{n}2\pi + \frac{k_2 v - m_2 n}{n}2\pi = 2\pi, \tag{32}$$

where m_1 and m_2 are the integers satisfying $1 \leq k_1 v - m_1 n \leq n$ and $1 \leq k_2 v - m_2 n \leq n$. Thus we have

$$(k_1 + k_2)v = (m_1 + m_2 + 1)n. \tag{33}$$

Since v and n have no common divisor except 1 for an indivisible structure, the smallest possible (integer) solution for k_1 and k_2 is $k_1 + k_2 = n$. However, we have

$$2 \leq k_1 + k_2 \leq n - 1 < n; \tag{34}$$

due to $1 \leq k_1 \leq (n-1)/2$ and $1 \leq k_2 \leq (n-1)/2$. Therefore, Eq. (33) can not hold, and hence $C_{k_1 v} \neq C_{k_2 v}$ holds for $k_1 \neq k_2$.

As there are in total $(n-1)/2$ elements for j ($\in \{1, \ldots, (n-1)/2\}$), and $(n-1)/2$ different values in Eq. (30), every cosine value in the list has been taken, but only once, by C_{jv} for an indivisible structure with n odd, which proves the lemma. □

Some examples are given in Fig. 6 for different v for the case $n = 9$. The solid lines links the points showing cosine values for C_{jv} ($j \in \{1, \ldots, 4\}$). The four points take different cosine values for indivisible structures ($v = 1, 2, 4$), and duplicate for the divisible structure ($v = 3$).

From Lemma 1, we must have the following relation from Eq. (30) to ensure that the relation in Eq. (28) always holds

$$v = p = \frac{n-1}{2}. \tag{35}$$

In other words, a dihedral star tensegrity structure is super stable if and only if it has odd number of struts (n odd), and the struts are as close to each other as possible ($v =$

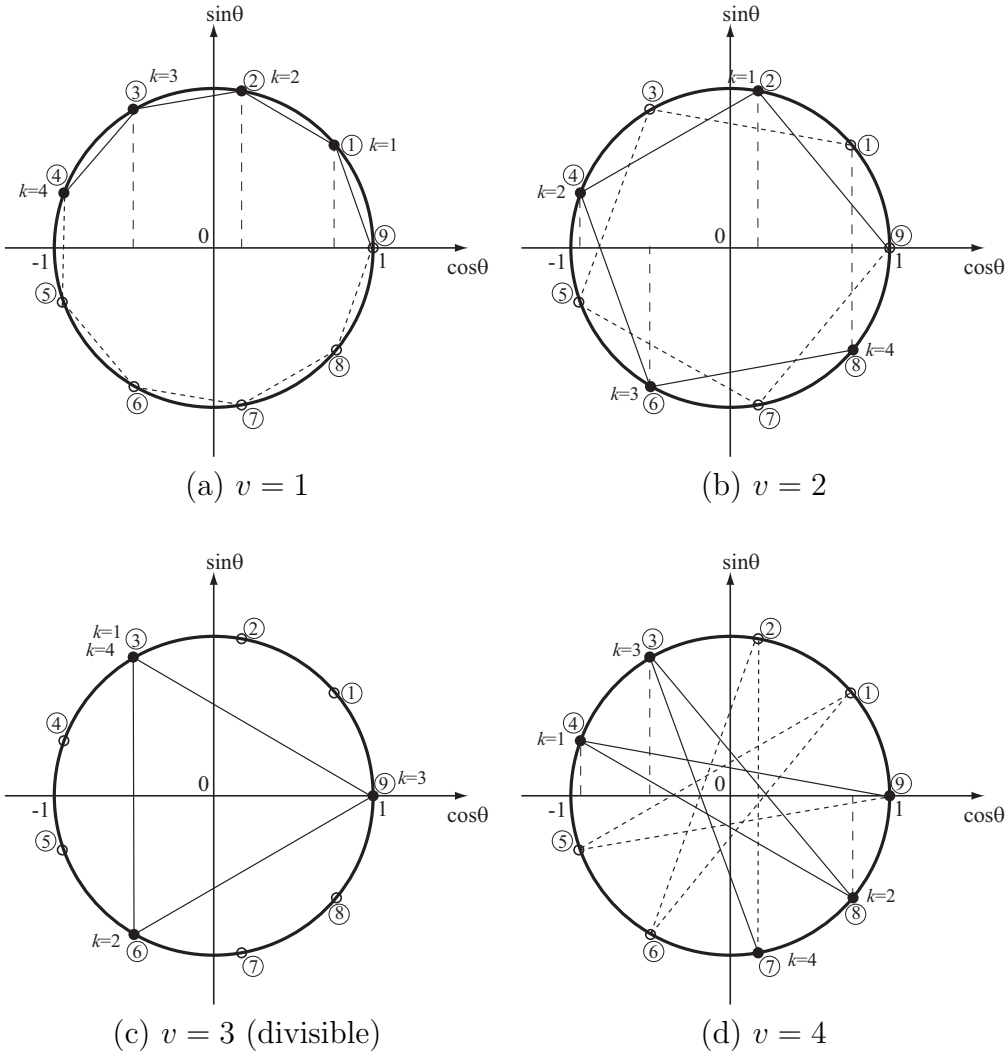

Fig. 6. Connectivity of boundary nodes in one circle through struts and vertical cables ($n = 9$). Every cosine value is taken only once, if the structure is indivisible, see the cases (a), (b) and (d). For the divisible case in (c), only part of the cosine values have been taken.

$(n-1)/2$). This is the necessary and sufficient condition for super stability of dihedral star tensegrity structures.

4.3 Prestress Stability

We have found the super stability condition for dihedral star tensegrity structures in the previous section. We show in this section through numerical calculation that some other structures, that are not super stable, can still be prestress stable if certain conditions are satisfied — a treatment that follows Zhang *et al.* (2008a).

A prestress stable structure has a positive definite reduced geometrical stiffness matrix

$$\mathbf{Q} = \mathbf{M}\mathbf{K}^G\mathbf{M}^{\mathrm{T}}, \tag{36}$$

where columns of $\mathbf{M}$ are the infinitesimal mechanisms of the structure, and $\mathbf{K}^G$ is the geometrical stiffness matrix defined by the tensor product of a 3×3 identity matrix $\mathbf{I}_3$

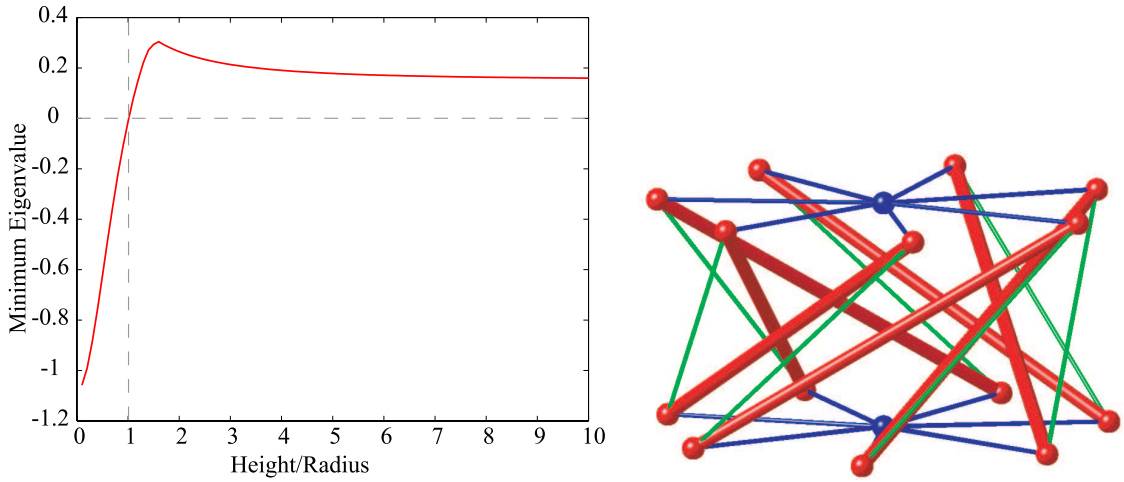

Fig. 7. Prestress stability of the dihedral star tensegrity structure $\mathbf{D}_7^1$. When the height/radius ratio is larger than 1.02, it is prestress stable with the positive minimum eigenvalue of the reduced stiffness matrix.

Table 1
Stability of dihedral star tensegrity structures $\mathbf{D}_n^v$, for $3 \leq n \leq 10$. 'S' denotes super stable; if the structure is prestress stable only when the height/radius ratio is larger than r, then this is indicated as '$\geq r$'; and if the structure is divisible, its substructures are given.

$v\backslash n$	3	4	5	6	7	8	9	10
1	S	≥ 0.46	≥ 0.65	≥ 0.87	≥ 1.02	≥ 1.18	≥ 1.30	≥ 1.43
2		$2\mathbf{D}_2^1$	S	$2\mathbf{D}_3^1$	≥ 0.32	$2\mathbf{D}_4^1$	≥ 0.57	$2\mathbf{D}_5^1$
3				$3\mathbf{D}_2^1$	S	≥ 0.11	$3\mathbf{D}_3^1$	≥ 0.29
4						$4\mathbf{D}_2^1$	S	$2\mathbf{D}_5^2$
5								$5\mathbf{D}_2^1$

and the force density matrix, $\mathbf{K}^G = \mathbf{I}_3 \otimes \mathbf{E}$ (Guest, 2006). The structure is prestress stable if and only if the minimum eigenvalue λ^Q of $\mathbf{Q}$ is positive.

As an example, Figs. 7, 8 and 9 plot the values of λ^Q against the ratios of height to radius (H/R) for the star tensegrity structures with dihedral symmetry $\mathbf{D}_7$. The force density matrix is calculated relative to the force density of vertical cables, or by assigning $q_v = 1$ alternatively without losing generality. The structure $\mathbf{D}_7^3$ is super stable and is thus always prestress stable; the structures $\mathbf{D}_7^1$ and $\mathbf{D}_7^2$ are not super stable, but it can be observed from Figs. 7 and 8 that they are prestress stable if the height/radius ratio is large enough.

These figures have the same appearance: the minimum eigenvalue of the reduced stiffness matrix increases sharply firstly, and then decreases with the increasing height/radius ratios. Finally, the minimum eigenvalue converges gradually to a *positive* value, such that the structure is prestress stable.

Table 1 shows the stability of star structures with $3 \leq n \leq 10$. It can be seen that every indivisible structure in this range can be prestress stable.

5. Discussion

This paper has presented the necessary and sufficient condition for super stability of

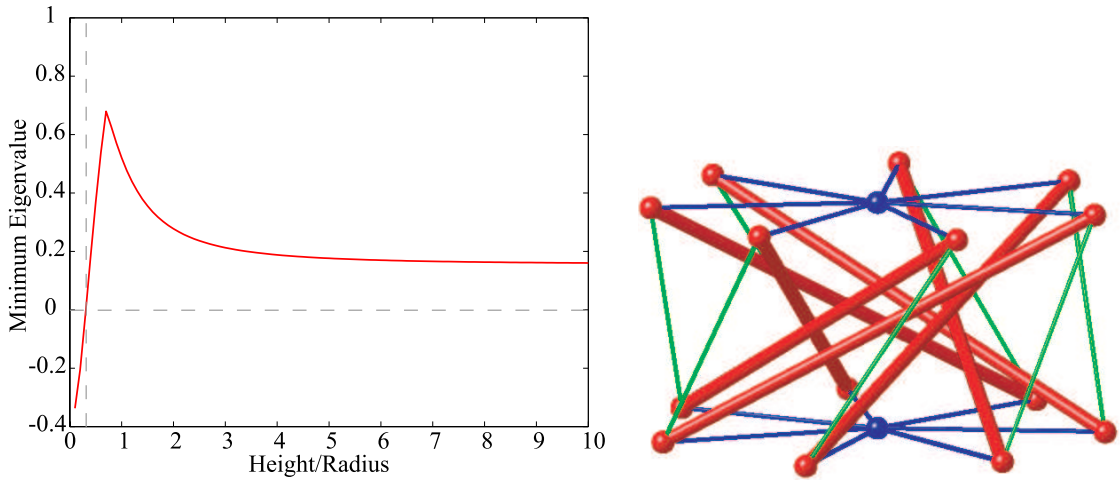

Fig. 8. Prestress stability of the dihedral star tensegrity structure $\mathbf{D}_7^2$. When the height/radius ratio is larger than 0.32, it is prestress stable with the positive minimum eigenvalue of the reduced stiffness matrix.

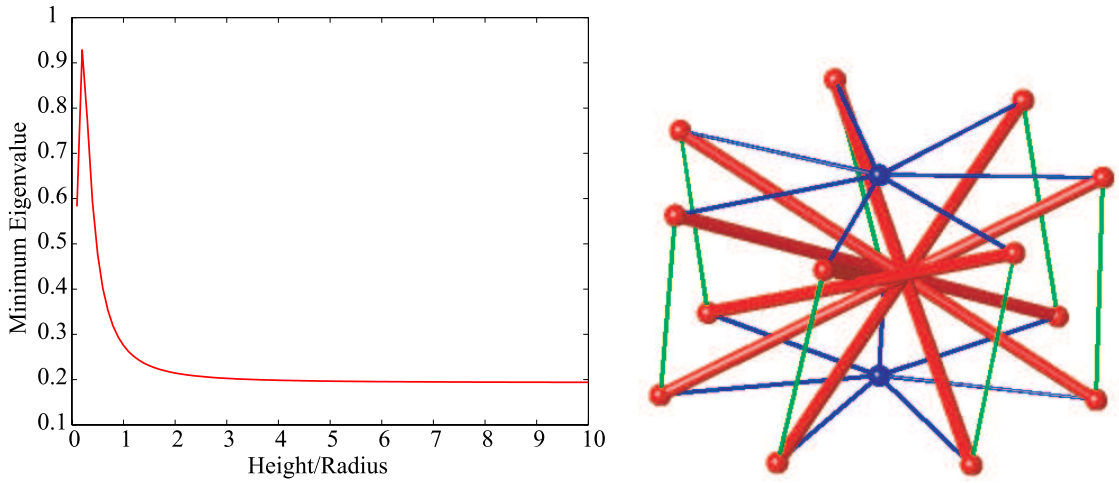

Fig. 9. Prestress stability of the dihedral star tensegrity structure $\mathbf{D}_7^3$. From the super stability condition for star structures, this structure is super stable, and hence, it is always prestress stable irrespective of the height/radius ratio.

dihedral star tensegrity structures — the structures are super stable if and only if they have odd number of struts, and the struts are as close to each other as possible. Furthermore, we conjecture that all indivisible dihedral star tensegrity are prestress stable if the height/radius ratio is large enough: numerical calculations have shown this to be true for all $3 \leq n \leq 100$, although only simpler cases $3 \leq n \leq 1000$ have been presented.

If the centre nodes of a star structure are connected by an additional 'centre' member, see for example the structure shown in Fig. 10, the new structure is also of dihedral symmetry. Numerical calculations show that the super stability condition and the conjectures on prestress stability for the structures without centre members also apply to these structures. However, any proof of their stability properties is complicated by the existence of an additional parameter, the distance between the centre nodes.

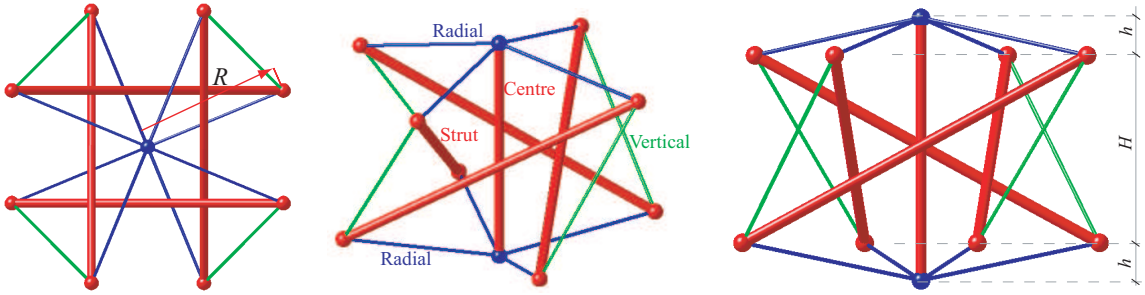

(a) top (b) perspective (c) side

Fig. 10. Dihedral star tensegrity structure with centre member. It has the same connectivity as the structure $\mathbf{D}_4^1$, except for the additional centre member connecting the two centre nodes. The parameter h denotes the distance between a center node to the closest centre of circle containing boundary nodes. The centre member is a strut when $h > 0$, a cable when $h < 0$, and there exists no prestress in the member when $h = 0$. This structure is prestress stable but not super stable as confirmed by numerical calculation.

Acknowledgement:
JYZ is grateful for financial support from The Kyoto University Foundation and the EPSRC while visiting the Department of Engineering at the University of Cambridge. RC is grateful for support from the EPSRC while visiting the Department of Engineering at the University of Cambridge, and support from NSF Grant No. DMS-0209595.

References

Altmann, S.L. and Herzig, P., Point-group Theory Tables. Clarendon Press, Oxford, 1994.

Kettle, S.F.A., Symmetry and Structure, 2nd ed. John Wiley & Sons Ltd, West Sussex, England, 1995.

Connelly, R., 1982. Rigidity and energy. Invent. Math. 66(1), 11–33.

Connelly, R. and Terrell, M., 1995. Globally rigid symmetric tensegrities. Structural Topology, 21, 59–78.

Guest, S.D., 2006. The stiffness of prestressed frameworks: a unifying approach. Int. J. Solids Struct., 43, 842–854.

Zhang, J.Y., Guest, S. and Ohsaki, M., 2008a. Symmetric prismatic tensegrity structures: Part I. configuration and stability. Int. J. Solids Struct., in press.

Zhang, J.Y., Guest, S. and Ohsaki, M., 2008b. Symmetric prismatic tensegrity structures: Part II. symmetry-adapted formulations. Int. J. Solids Struct., in press.

Zhang, J.Y. and Ohsaki, M., 2006. Adaptive force density method for form-finding problem of tensegrity structures. Int. J. Solids Struct., 43(18-19), pp. 5658–5673.

Zhang, J.Y. and Ohsaki, M., 2006. Stability conditions for tensegrity structures. Int. J. Solids Struct., 44(11-12), pp. 3875–3886.